

# Terrain matching localization for hybrid underwater vehicle in the Challenger Deep of the Mariana Trench\*

Jian WANG<sup>†1,2</sup>, Yuan-gui TANG<sup>†‡1,2</sup>, Chuan-xu CHEN<sup>†‡3</sup>, Ji-xu LI<sup>1,2</sup>, Cong CHEN<sup>1,2</sup>  
 Ai-qun ZHANG<sup>1,2,3</sup>, Yi-ping LI<sup>1,2</sup>, Shuo LI<sup>1,2</sup>

<sup>1</sup>State Key Laboratory of Robotics, Shenyang Institute of Automation, Chinese Academy of Sciences, Shenyang 110016, China

<sup>2</sup>Institutes for Robotics and Intelligent Manufacturing, Chinese Academy of Sciences, Shenyang 110016, China

<sup>3</sup>Institute of Deep-sea Science and Engineering, Chinese Academy of Sciences, Sanya 572000, China

<sup>†</sup>E-mail: wangjian3@sia.cn; tyg@sia.cn; chencx@idsse.ac.cn

Received Oct. 11, 2019; Revision accepted Jan. 14, 2020; Crosschecked Apr. 1, 2020

**Abstract:** The maximum ocean depth so far reported is about 11 000 m, and is located in the Mariana Trench in the Western Pacific Ocean. The hybrid unmanned underwater vehicle, Haidou, is developed to perform scientific survey at the deepest parts of the Earth oceans. For vehicles working at the full-ocean depth, acoustic positioning is the most effective and popular method. The 11 000 m class acoustic positioning system is relatively massive and complex, and it requires specialized research vessels equipped with compatible acoustic instruments. As a compact testbed platform, it is impractical for Haidou to carry an LBL/USBL beacon with its large volume and weight. During the descent to about 11 000 m, horizontal drift could not be eliminated because of the hydrodynamics and uncertain ocean currents in the sea trials. The maximum depth recorded by Haidou is 10 905 m, and determining the precise location of the deepest point is challenging. With the bathymetric map produced by a multibeam sonar, the terrain contour matching (TERCOM) method is adopted for terrain matching localization. TERCOM is stable in providing an accurate position because of its insensitivity to the initial position errors. The final matching results show the best estimate of location in the reference terrain map.

**Key words:** Hybrid underwater vehicle; Full-ocean depth; Challenger Deep; Mariana Trench; Terrain contour matching  
<https://doi.org/10.1631/FITEE.1900556>

**CLC number:** TP242.6; TP273

## 1 Introduction

Challenger Deep is an east-west trending basin located in the Mariana Trench (Fig. 1), within the territorial waters of the Federated States of Micronesia. There have been several attempts throughout history to determine the maximum depth of the Earth oceans. There are basically two methods, i.e.,

echosounder-based measurement and direct measurement using in-situ pressure sensors (Gardner et al., 2014). To the best of our knowledge, there are only four unmanned underwater vehicles capable of diving to the full-ocean depth, namely, KAIKO ROV and UROV11K ROV of Japan (Kyo et al., 1995; Nakajoh et al., 2018), Nereus HROV of the United States (Bowen et al., 2009), and Haidou ARV of China (Tang et al., 2019). Unfortunately, KAIKO ROV, UROV11K ROV, and Nereus HROV have been lost in deep-sea dives. There seem to be numerous challenges and unknown risks in full-ocean depth vehicle development and sea trials.

The hybrid unmanned underwater vehicle, Haidou, was developed for scientific survey to the depth of 11 000 m. The initial goal of the Haidou

<sup>‡</sup> Corresponding authors

\* Project supported by the National Key R&D Program of China (Nos. 2018YFC0308804 and 2016YFC0300800) and the Strategic Priority Research Program of Chinese Academy of Sciences (No. XDB06050200)

 ORCID: Yuan-gui TANG, <https://orcid.org/0000-0002-0067-3278>; Chuan-xu CHEN, <https://orcid.org/0000-0001-8823-8221>

© Zhejiang University and Springer-Verlag GmbH Germany, part of Springer Nature 2020

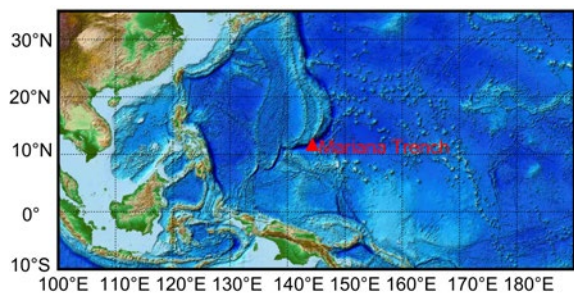


**Fig. 1 General location of the Mariana Trench**

Project was to develop the key technologies for the full-ocean depth. To validate the technologies in the deep-ocean environment, Haidou was designed as a testbed platform. However, most full-ocean depth equipment is customized, expensive, and bulky. Referring to KAIKO, UROV11K, and Nereus, specially developed acoustic positioning systems were employed for localization. Looking up the available documents, acoustic positioning was the only application case at the deepest ocean of the world. However, due to the limitations of weight, volume, battery energy, and research budget, Haidou was not integrated with the long baseline (LBL)/ultra-short baseline (USBL) beacon for precise localization. Therefore, how to locate the survey area is the problem that we have to cope with. For the study of the Challenger Deep, besides making claims of the maximum detected depth value, it is significant to research the coordinates of the maximum depth.

At present, inertial navigation systems (INSS) have been widely used in underwater vehicles even for the under polar ice environment (Li et al., 2011). Since the INS error inevitably accumulates over time, assisting measures should be taken, such as acoustic USBL aided SINS (USBL SINS) and ocean geophysics aided SINS (geomagnetic/terrain/gravity SINS). If an a priori map of the survey field is accessible, measurement of geophysical information can be implemented to estimate the vehicle position. Underwater vehicle navigation based on topographical data has been successfully demonstrated (Bergem et al., 1993). In this system, depths are measured throughout the mission by a multibeam sonar to produce an accurate profile of the seafloor. The multibeam sonar profile is matched against the a priori map to determine the vehicle position. Terrain matching localization is a promising technique for

obtaining the estimated position of Haidou with the topographic information.

In recent years, the wide application potential of terrain matching localization in the underwater environment has attracted the attention of scholars around the world. The terrain matching localization system does not need any other extra equipment. It is invisible and has no cumulative time error. Terrain contour matching (TERCOM), iterated closest contour point (ICCP), and Sandia inertial terrain assisted navigation (SITAN) are classic terrain matching algorithms in underwater navigation. The SITAN algorithm adopts a set of extended Kalman filters (EKFs) to deal with the difference between the expected topographical information and the measured topographical information to estimate the position. However, it takes a long search time, and sometimes misses the matching position for a large search sequence. In addition, the SITAN algorithm requires a precise initial position (Yuan et al., 2012). The ICCP algorithm adopts a rigid transformation to match the contour lines, and can achieve high accuracy with a small initial position error. Nevertheless, it may lead to a matching failure for a large initial position error (Wang HB et al., 2018). The TERCOM algorithm determines the location by calculating the correlation of the background terrain and the surveyed bathymetric sequence. The TERCOM algorithm has the advantages of easy implementation, fast calculation, and good stability. The highlight of TERCOM is that it is insensitive to the initial errors (Zhao et al., 2015; Han et al., 2017).

In this study, we propose a terrain matching method to settle the localization problem without an acoustic positioning system at the maximum depth of the Earth oceans. To achieve this, we propose a high-precision pressure-depth conversion for bathymetry calculation, which provides data support for the maximum depth value recorded by Haidou. Terrain characteristic analysis is necessary. It is meaningful to select the appropriate terrain matching region based on topographic information. The key of the localization method is to match the bathymetric data collected by Haidou against the a priori multibeam terrain map with the TERCOM algorithm. This approach has been applied in sea trials in the Challenger Deep of the Mariana Trench. Matching results provide the best estimate of position of the survey area and the global coordinates of the deepest recorded point.

## 2 Full-ocean depth localization problem formulation

In this section, we give a brief description of the Haidou vehicle, and then introduce the localization problem at the full depth of the ocean.

### 2.1 Haidou overview

The Haidou vehicle was designed as a compact vehicle that can perform scientific research with in-situ sensors and a high-definition (HD) camera at the full-ocean depth of 11 000 m (Fig. 2). Basic parameters of Haidou ARV are listed in Table 1. The dimensions of Haidou are 0.85 m (length) $\times$ 0.4 m (width) $\times$ 1.2 m (height). Its weight is 260 kg in air. With a mission controller, the vehicle could work as an autonomous underwater vehicle (AUV) for broad-area survey. With a single microfiber optic cable of 0.4 mm diameter, the vehicle can be operated as a remotely-operated vehicle (ROV) capable of close-up imaging of interested scenes and high-quality tele-operation. Haidou vehicle is equipped with an HD camera and two LED lights for observation. The survey sensors include a Keller PA-33X pressure sensor, a Sea-Bird SBE49 CTD sensor, and a 400-kHz single-beam echosounder. The motion of Haidou is accomplished by four propulsion DC-brushless motors. Two vertical thrusters are used for depth control, and two other thrusters are used for horizontal cruising. The large metacentric height of the vehicle provides passive stability in roll and pitch. The fixed vertical tail provides passive hydrodynamic stability in heading. Haidou is a portable vehicle system that can be easily launched without dynamic positioning of the ship.

### 2.2 Localization problem at the full depth of the ocean

Acoustic systems are the standard for precise underwater positioning. Beacons are placed on vehicles or areas of interest. Position fixes are calculated with the LBL or USBL technique. In general, the acoustic positioning system is reliable with bounded errors, but the range is limited by acoustic propagation of the transponder and beacons. For the range of the full-ocean depth, the acoustic units are bulky. The thick hull is required to resist the gigantic pressure of sea water. In addition, there is no market product, and

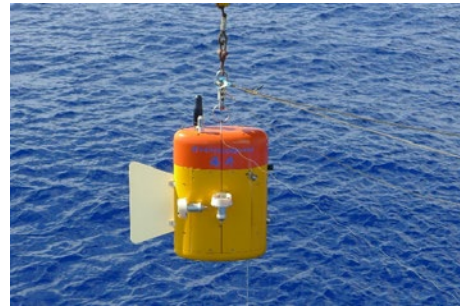


**Fig. 2 Haidou hybrid underwater vehicle designed to work at the full-ocean depth of 11 000 m**

**Table 1 Basic parameters of Haidou ARV**

Parameter	Value/Illustration
Maximum working depth (m)	11 000
Weight in air (kg)	260
Dimensions (m $\times$ m $\times$ m)	0.85 $\times$ 0.4 $\times$ 1.2
Operation models	Autonomous and remotely-operated
Sensors	An SBE 49 CTD sensor, a PA-33X pressure gauge, and a single-beam echosounder
Load capacity (kg)	5
Sailing speed (knot)	1
Battery	Rechargeable lithium ion battery (2 kW $\cdot$ h)
Thrusters	Two in horizontal and two in vertical
Unpowered descent and ascent speed	No less than 50 m/min on average
Other supporting equipment	A fiber optic compensator near surface, a deck control and display station, and a transport platform

the 11 000 m class acoustic positioning system is customized, time-consuming, and expensive. From the available literature, acoustic positioning is the only application case of full-ocean depth positioning.

As described in Section 2.1, Haidou was designed as a compact testbed platform to verify the key technologies at the full depth of the ocean. It is undesirable and impractical for Haidou to carry an LBL/USBL beacon with a large size and weight. During a descent to about 11 000 m, horizontal drift is affected by hydrodynamics and uncertain ocean currents. Localization of the survey area is tough, and determining the precise location of the recorded deepest point is even more challenging. If an accurate a priori map of the environment is available, bathymetry can be used to estimate the vehicle position.

### 3 Terrain matching localization method

In this section, we describe terrain characteristic analysis and high-precision depth calculation with in-situ sensors, and then introduce the TERCOM method.

#### 3.1 Matching terrain characteristic analysis

False terrain matching localization may occur if the matching terrain is flat or repetitive without uniqueness. It is vital to classify the terrain and determine the appropriate matching region. In a terrain matching system, terrain elevation standard deviation and topographic information entropy are often used to reflect the inherent characteristics of the terrain.

Supposing that a region is divided into  $m \times n$  grids and that  $z(i, j)$  is the topographic elevation of point  $(i, j)$ , the terrain inherent characteristic parameters can be defined as follows:

##### 1. Terrain elevation standard deviation

Terrain elevation standard deviation reflects the topographic fluctuation intensity of the terrain. The larger the standard deviation of the terrain elevation in the region is, the more dramatically the terrain fluctuates.

$$\bar{z} = \frac{1}{mn} \sum_{i=1}^m \sum_{j=1}^n z(i, j), \quad (1)$$

$$D(z) = \frac{1}{m(n-1)} \sum_{i=1}^m \sum_{j=1}^n [z(i, j) - \bar{z}]^2, \quad (2)$$

$$\sigma = \sqrt{D(z)}, \quad (3)$$

where  $\bar{z}$  represents the mean of the terrain elevation,  $D(z)$  the variance of the topographic elevation, and  $\sigma$  the terrain elevation standard deviation.

##### 2. Topographic information entropy

Topographic information entropy reflects the amount of elevation information in the region, and can be used to depict a terrain feature. If the elevation value of a region changes rapidly, the fluctuation changes are large, the topography is specific, and the calculated local topographic entropy is small. Otherwise, the calculated topographic entropy is large.

$$H_f = - \sum_{i=1}^m \sum_{j=1}^n p_{ij} \log p_{ij}, \quad (4)$$

$$p_{ij} = \frac{z(i, j)}{\sum_{i=1}^m \sum_{j=1}^n z(i, j)}, \quad (5)$$

where  $H_f$  represents the terrain entropy and  $p_{ij}$  the normalized topographic elevation of the given point  $(i, j)$ .

#### 3.2 High-precision depth measurement and calibration with in-situ sensors

##### 3.2.1 Sensors for depth measurement

Sensors carried by the Haidou vehicle for sea-floor depth measurement include a Keller PA-33X pressure sensor, a Sea-Bird SBE49 CTD sensor, and a single-beam echosounder. The specific parameters of the PA-33X pressure, SBE49 CTD sensor, and single-beam echosounder are shown in Tables 2, 3, and 4, respectively.

**Table 2 Specifications of the Keller PA-33X pressure sensor**

Parameter	Value
Pressure endurance (MPa)	120
Weight in air (g)	240
Accuracy	0.01%FS
Resolution	0.002%FS
Storage/Operating temperature range (°C)	-40-120

FS: full scale

**Table 3 Specifications of the Sea-Bird SBE49 CTD sensor**

Property	Temperature (°C)	Conductivity (s/m)	Pressure (dbar)
Measurement range	-5-35	0-9	0-10 500
Accuracy	±0.002	±0.0003	±0.1%FS
Typical stability	0.0001	0.000 05 oceanic water	0.002%FS
Resolution	0.0002 per month	0.0003 per month	0.05%FS per year

FS: full scale. 1 dbar=1×10<sup>4</sup> Pa

**Table 4 Specifications of the single-beam echosounder**

Parameter	Value
Maximum working depth (m)	11 000
Weight in air (kg)	2.8
Frequency (kHz)	400
Beam width (°)	10
Maximum range (m)	100
Resolution (m)	0.3

### 3.2.2 Depth calibration

Calculation of the pressure depth in the ocean is based on the hydrostatic equation:

$$p = \rho gh, \quad (6)$$

where  $g$  is the local acceleration due to the gravity,  $h$  the depth,  $\rho$  the density, and  $p$  the pressure. In the ocean, the water column is not well-distributed. The density value is different at different locations and in different times. The value of acceleration due to the gravity varies with the depth and latitude. Deep-sea scientists are aware of the importance and difficulty of accurate depth calculations.

The integral form of the hydrostatic equation is

$$\int_0^z g dz = \int_0^p v(s, t, p) dp, \quad (7)$$

where  $v(s, t, p)$  is the in-situ specific volume of seawater with salinity  $s$  at temperature  $t$  under pressure  $p$ .

Before the development of a full-ocean depth vehicle or lander, there were no efficient tools for direct in-situ measurement of a specific volume of seawater and its density. Simplification and approximation of Eq. (7) was conducted, and the practical formula was proposed (Fofonoff and Millard, 1983). By solving Eq. (7), Fofonoff and Millard (1983) calculated the depth from the pressure and the latitude by the following equation:

$$Z = Z_s(p, \theta) + \frac{\Delta D}{9.8}, \quad (8)$$

where  $Z_s(p, \theta)$  is a universal expression for calculating depth in the “standard ocean” (an ideal medium in temperature  $T=0$  °C and salinity  $S=35$  psu) and  $\theta$  is the latitude. The term  $\Delta D$ , called geopotential anomaly, accounts for the difference in the temperature and salinity structure from the “standard ocean.”

The complete formulation of  $Z_s(p, \theta)$  is expressed as

$$H_i = \frac{\{(A_1 p_i + B_1) p_i - C_1\} p_i + D_1}{F(\theta, p_i)}, \quad (9)$$

where  $A_1=-1.82 \times 10^{-15}$ ,  $B_1=2.279 \times 10^{-10}$ ,  $C_1=2.2512 \times 10^{-5}$ , and  $D_1=9.72659$ .

$$F(\theta, p_i) = A_2[1 + (B_2 + C_2 \sin^2 \theta) \sin^2 \theta] + D_2 p_i, \quad (10)$$

where  $A_2=9.780318$ ,  $B_2=5.2788 \times 10^{-3}$ ,  $C_2=2.36 \times 10^{-5}$ , and  $D_2=1.092 \times 10^{-6}$ .

This procedure is an algorithm adopted in the SBE CTD instrument for pressure-to-depth conversion, and this procedure is commonly used, here abbreviated as F-M.

Haidou vehicle is capable of measuring the full-ocean density profile (a function of salinity, temperature, and pressure) in situ. So, there is no need to use the traditional F-M practical formula for simplification and approximation. Instead, we directly calculate the depth by solving the integral form of the hydrostatic equation.

The depth value  $H_i$  is described by

$$H_i = \sum_{i=1}^M h_i, \quad (11)$$

where  $h_i$  represents the depth change between  $p_i$  and  $p_{i-1}$ , and can be calculated by

$$h_i = \frac{p_i - p_{i-1}}{\rho_i g_i}, \quad (12)$$

where  $\rho_i$  is the density and  $g_i$  the gravity at pressure  $p_i$  in the water column.

According to Sea-Bird Electronics Inc. (2007), the density is influenced by salinity, temperature, and pressure, expressed as

$$\rho_i = \frac{A + B + C + D}{1 - \frac{P_i}{E + F + G + H + I + J + K + M}}, \quad (13)$$

where

$$\left\{ \begin{array}{l} A = A_0 + A_1 t_i + A_2 t_i^2 + A_3 t_i^3 + A_4 t_i^4 + A_5 t_i^5, \\ B = (B_0 + B_1 t_i + B_2 t_i^2 + B_3 t_i^3 + B_4 t_i^4) s_i, \\ C = (C_0 + C_1 t_i + C_2 t_i^2) s_i^{1.5}, \\ D = D_0 s_i^2, \\ E = E_0 + E_1 t_i + E_2 t_i^2 + E_3 t_i^3 + E_4 t_i^4, \\ F = (FQ_0 + FQ_1 t_i + FQ_2 t_i^2 + FQ_3 t_i^3) s_i, \\ G = (G_0 + G_1 t_i + G_2 t_i^2) s_i^{1.5}, \\ H = (H_0 + H_1 t_i + H_2 t_i^2 + H_3 t_i^3) p_i, \\ I = (I_0 + I_1 t_i + I_2 t_i^2) s_i p_i, \\ J = J_0 s_i^{1.5} p_i, \\ K = (K_0 + K_1 t_i + K_2 t_i^2) p_i^2, \\ M = (M_0 + M_1 t_i + M_2 t_i^2) s_i p_i^2. \end{array} \right.$$

The specific coefficients and the formula to calculate the salinity with conductivity, temperature, and pressure are given in Sea-Bird Electronics Inc. (2007).

According to McDougall and Barker (2011), the acceleration due to the gravity in the ocean is related to the latitude and depth. With a known latitude  $\theta$  and a calculated  $H_{i-1}$ ,  $g_i$  is calculated by

$$g_i = g_0 \{1 + [A_3 + (B_3 - 5 \sin^2 \theta) \sin^2 \theta]\} (1 - C_3 H_{i-1}), \quad (14)$$

where  $g_0=9.780327$ ,  $A_3=5.2792 \times 10^{-3}$ ,  $B_3=2.32 \times 10^{-5}$ , and  $C_3=2.26 \times 10^{-7}$ .

### 3.3 Terrain contour matching based on the mean square difference

TERCOM was originally developed for aerial platforms and first deployed in cruise missiles. It is one of the most popular matching algorithms and has been applied successfully in practice. TERCOM performs a batch correlation of the measured profile against the a priori map rather than individual recursive measurement, thus reducing sensitivity to the initial position errors. The generally applied matching rules of TERCOM are cross correlation (COR), mean absolute difference (MAD), and mean square difference (MSD) (Wang KD and Yong, 2010). The definitions are as follows:

$$\text{COR}(x, y) = \frac{1}{N} \sum_{i=1}^N d_M(i) d_{BT}(x, y, i), \quad (15)$$

$$\text{MAD}(x, y) = \frac{1}{N} \sum_{i=1}^N |d_M(i) - d_{BT}(x, y, i)|, \quad (16)$$

$$\text{MSD}(x, y) = \frac{1}{N} \sum_{i=1}^N [d_M(i) - d_{BT}(x, y, i)]^2, \quad (17)$$

where  $d_M$  is the measured depth sequence using in-situ sensors,  $d_{BT}$  the background terrain map, and  $N$  the matching length.

COR may lead to a mismatch to some extent. MSD correlation matching algorithm is an effective approach for ascertaining the most relevant position in the terrain map. Since the accuracy of MSD is slightly higher than those of COR and MAD, MSD is used in this study. The position where MSD is minimum fulfills the best matching with the background terrain map.

## 4 Sea trials and terrain matching localization results

### 4.1 Sea trials

Sea trials were conducted in September and October 2018 from the R/V TANSUOYIHAO in the Challenger Deep of the Mariana Trench in the Western Pacific Ocean.

#### 4.1.1 Reference terrain map with a multibeam sonar

The R/V TANSUOYIHAO multibeam sonar (KONGSBERG EM122) was used to produce maps of the seafloor during the cruise. The EM122 is a 12-kHz multibeam system that produces bathymetric data and seafloor acoustic backscatter imaging in the water depth up to 11 000 m. Fig. 3 shows parts of the EM122 bathymetric data around the Challenger Deep in a three-dimensional (3D) view. The reference map stretches about 23.8 km east to west and 17.7 km south to north, covering an area of about 421 km<sup>2</sup> with a 20-m resolution. The bathymetric data varies from 8346 m to 10 928 m. The bathymetric contour of the reference map is shown in Fig. 4. Triangle in Fig. 4 represents the deepest point of the Challenger Deep from multibeam bathymetric data.

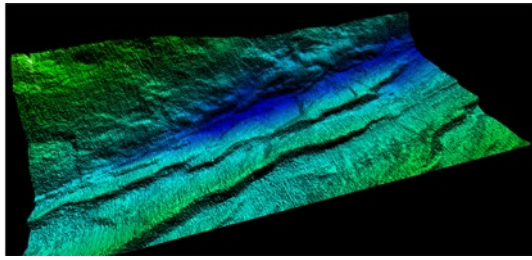


**Fig. 3** Parts of the EM122 bathymetric data around the Challenger Deep in a three-dimensional view

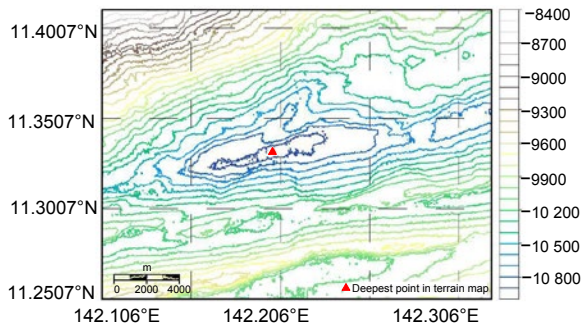


**Fig. 4** Bathymetric contour of the reference terrain map

#### 4.1.2 Terrain matching region selection

To determine a suitable region for terrain matching localization, the reference map was divided into 44×60 grids. Then, the terrain elevation standard deviation and topographic information entropy of each block were calculated.

The terrain elevation standard deviation of 44×60 grid areas is shown in Fig. 5. The light color regions represent where the terrain matching algorithm is more favorable and terrain suitability is better. Topographic change in the area containing the deepest point is small, indicating that the area is unsuitable for terrain matching. In the northeast direction near the deepest point, the high standard deviation value illustrates that the terrain is undulating.

The topographic information entropy of the 44×60 grid areas is shown in Fig. 6. Light color parts indicate where the regions are poor in topography information and unsuitable for terrain matching localization. Dark color parts indicate large entropy regions that are rich in topography information and suitable for terrain matching localization. The topographic entropy implies that the region in the northeast direction near the deepest point contains a lot of elevation information.

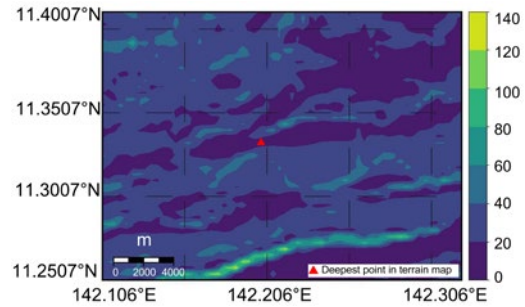


**Fig. 5** Terrain elevation standard deviation of 44×60 grid areas

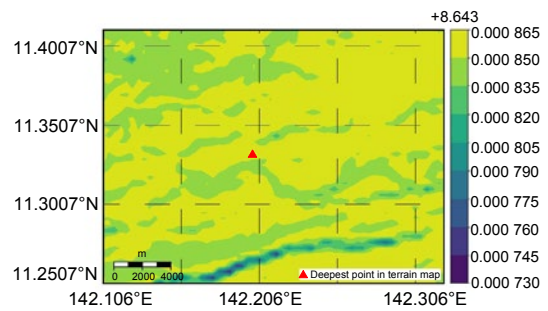


**Fig. 6** Topographic information entropy of 44×60 grid areas

Based on the terrain elevation standard deviation and topographic information entropy analysis, the launch point and the terrain matching region are selected. The selected launch point must contain sufficient bathymetric information, and the closer to the deepest point, the better. The terrain matching region can be large because the landing point drifts from the launch point after several hours of deep dive. As shown in Fig. 7, the selected launch point is located in the northeast direction of the deepest point in the terrain map. The selected matching region stretched about 5.8 km east to west and 3.7 km south to north. The region could supply decent bathymetric information for the terrain matching method.

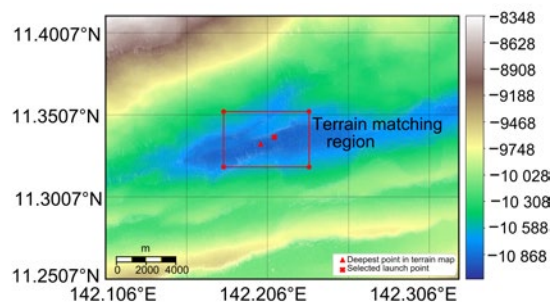


**Fig. 7** Terrain matching region selected from the reference terrain map

4.1.3 High-precision seafloor depth calculation with in-situ sensors

The measured conductivity and temperature of the whole water column are shown in Fig. 8. From Sea-Bird Electronics Inc. (2007) and McDougall and Barker (2011), the salinity, density, and gravity acceleration could be calculated.

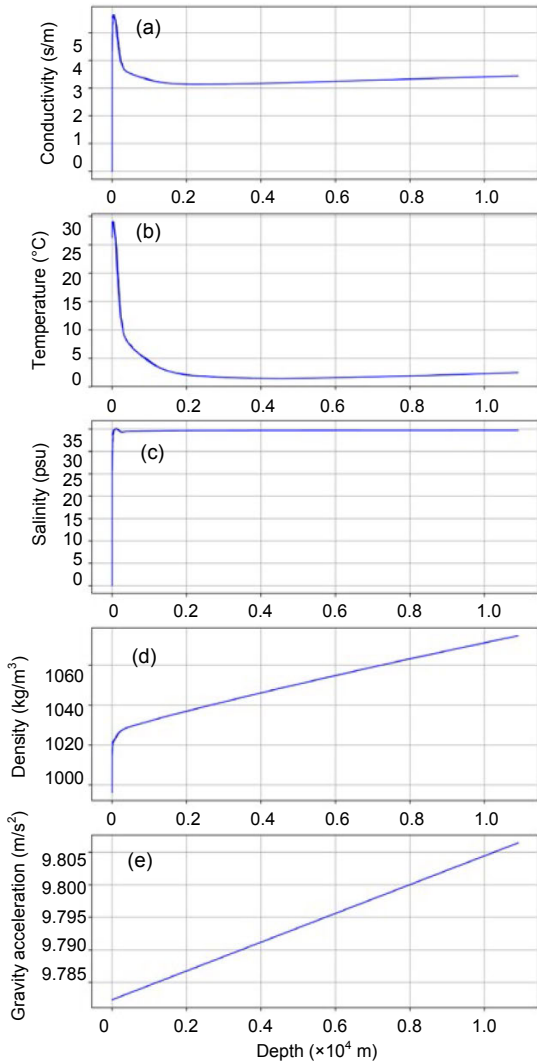


Fig. 8 Measured conductivity (a) and temperature (b) by SBE49 CTD, calculated salinity (c), density (d), and gravity acceleration (e)

The high-precision calibrated sailing depth of the Haidou vehicle during the whole dive is shown in Fig. 9. The descent time was about 3 h and 35 min, and the ascent time was about 3 h and 16 min. It took about 3 h to carry out the scientific investigation near the seafloor.

The bathymetric data consists of the depth measurement below the water surface and the altitude measurement above the seafloor. The vehicle sailed at a given altitude above the seafloor. The seafloor depth could be obtained by fusing the calibrated sailing depth with the sailing altitude from the single-beam echosounder (Fig. 10).

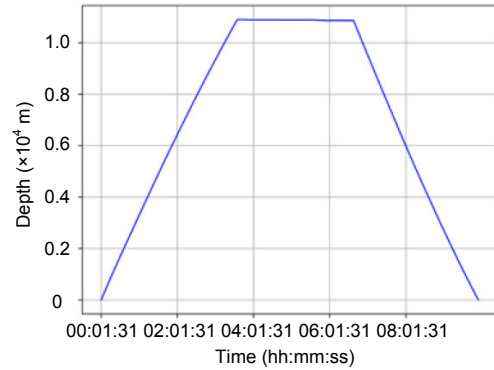


Fig. 9 Calibrated sailing depth of Haidou during the whole dive

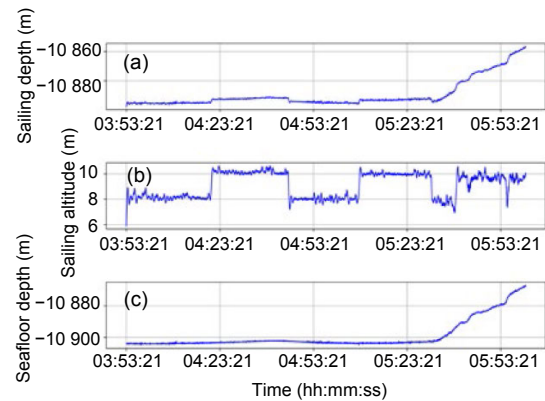


Fig. 10 Seafloor depth (c) obtained by fusing the sailing depth (a) with the sailing altitude (b)

4.1.4 Bathymetric survey results of Haidou

The Haidou hybrid underwater vehicle not only could be manually tele-operated from the ship, but also automatically works with an onboard computer. Normally, when Haidou is run automatically, it is set at a constant-depth or a constant-altitude mode like most AUVs. The planned trajectory was a U pattern. To sail near the seafloor given the rugged terrain in the Mariana Trench, the Haidou vehicle was set to work in a constant-altitude mode. On one hand, it could track the terrain well; on the other hand, it could avoid a collision.

During the survey near the seafloor, the real-time perception data transmitted to the ship indicated that the explored terrain was flat. The real-time video taken by the HD camera proved that as well (Fig. 11). Hence, it is infeasible to obtain characteristic values for the terrain with a small gradient.



**Fig. 11** HD camera image displaying that the exploring terrain of the U pattern trajectory is relatively flat

In accordance with the multibeam bathymetric data, there were topographic fluctuations in the northwest direction. Thanks to the micro optical fiber, the new desired heading command was sent and executed by the onboard computer. With the increasing number of measurement points, the estimate of position became more reliable. Subsequently, the depth value changed rapidly. Rocks and steep slopes appeared one after another in the video images (Figs. 12 and 13).



**Fig. 12** Rocks appearing in the camera when the Haidou vehicle is tele-operated to move in a northwest direction

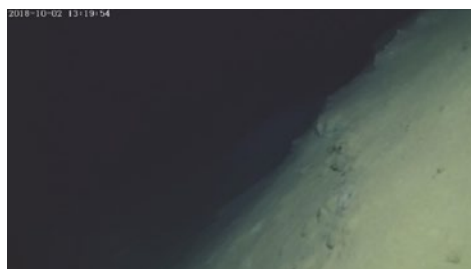


**Fig. 13** Steep slopes appearing when the Haidou vehicle continues to sail northwest

The sailing trajectory in a relative coordinate frame is shown in Fig. 14. The 3D trajectory is depicted in Fig. 15. As can be seen, the seafloor depth fluctuation is small in the U pattern trajectory. When the sailing heading is modified to the northwest, the seafloor depth changes dramatically, providing the topographic characteristics of terrain matching localization.

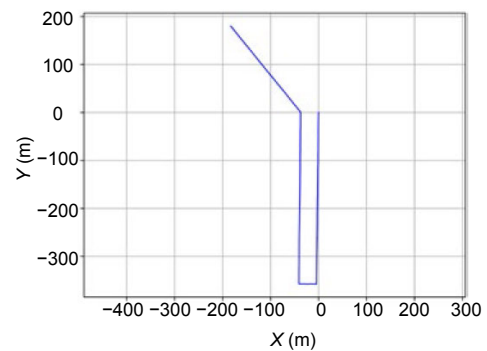


**Fig. 14** Sailing trajectory in a relative coordinate frame

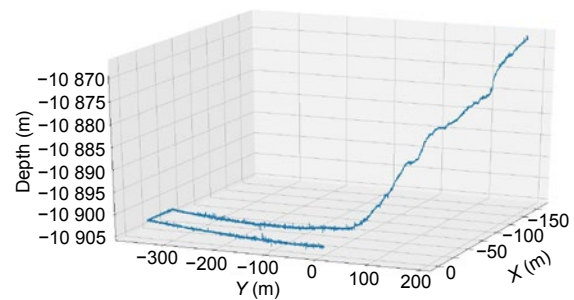


**Fig. 15** Three-dimensional trajectory demonstrating the depth fluctuations

#### 4.2 Terrain matching localization results

The matching region stretched about 5.8 km east to west and 3.7 km south to north. To obtain the best estimate of position, the whole region was searched. The search interval was equivalent to the map resolution. The Haidou-measured seafloor depth and the bathymetric data of the terrain matching region were processed in batches to calculate the corresponding MSD values. Based on TERCOM, the position where the MSD value was minimum fulfilled the best matching. As can be seen from Fig. 16, the matched position with the minimum MSD value made the multibeam bathymetric data consistent with the Haidou-measured depth. Generally, due to the uncertain sound velocity in the whole water column, the

multibeam bathymetric data was several meters deeper than the actual depth. The matched results provided more accurate in-situ depth measurement to calibrate the bathymetric data of the multibeam sonar.

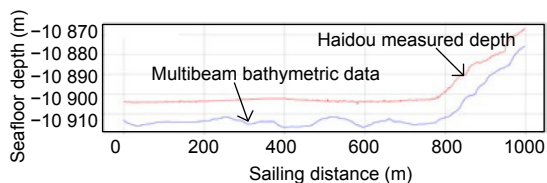


Fig. 16 Matched depth data based on MSD rules

The matched results are displayed in Fig. 17. The cross marker represents the launch point. The Haidou vehicle was launched at  $142^{\circ}12.583'E$ ,  $11^{\circ}20.227'N$  from the vessel. The initial position of the matched trajectory was  $142^{\circ}12.853'E$ ,  $11^{\circ}20.339'N$ . The horizontal distance between the launch point and the initial trajectory point was 533 m, meaning that the Haidou vehicle shifted approximately 533 m in the horizontal direction when it dived about 11 000 m to the seafloor in a vertical direction. The deepest point recorded by Haidou at the Challenger Deep represented with the star marker was located at  $142^{\circ}12.852'E$ ,  $11^{\circ}20.282'N$  with a depth of 10 905 m.

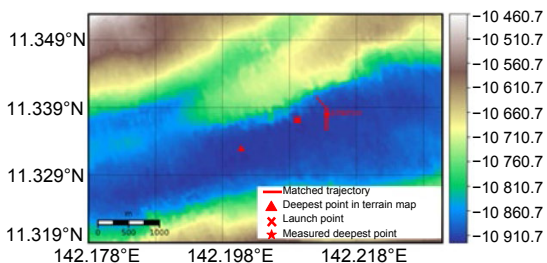


Fig. 17 Matched results in the reference terrain map

## 5 Conclusions

The Haidou hybrid underwater vehicle has been one of the few vehicles that are capable of diving the full-ocean depth. Because of a lack of an acoustic positioning system, a terrain matching localization method has been proposed. The sea trials have been conducted in the Mariana Trench, where the Haidou vehicle succeeded in reaching the seafloor. Based on the TERCOM MSD rules, the matching results showed the best estimate of position in the multibeam terrain map. The recorded deepest point of the sea

trials at the Challenger Deep was located at  $142^{\circ}12.852'E$ ,  $11^{\circ}20.282'N$  with a depth of 10 905 m. The collected video images and survey data in company with the matched global coordinates contributed to scientific exploration at the deepest area of the Earth oceans.

## Contributors

Yi-ping LI and Shuo LI supervised the project. Yuan-gui TANG designed the research. Jian WANG and Chuan-xu CHEN processed the data. Chuan-xu CHEN made visual presentation. Ji-xu LI and Cong CHEN participated in validation. Jian WANG drafted the manuscript. Ai-qun ZHANG helped organize the manuscript. Jian WANG revised and finalized the paper.

## Acknowledgements

Authors gratefully acknowledge the Haidou team for their creative and intensive efforts, and for the encouragement, help, and support of all members of R/V TANSUOYIHAO.

## Compliance with ethics guidelines

Jian WANG, Yuan-gui TANG, Chuan-xu CHEN, Ji-xu LI, Cong CHEN, Ai-qun ZHANG, Yi-ping LI, and Shuo LI declare that they have no conflict of interest.

## References

- Bergem O, Andersen CS, Christensen HI, 1993. Using match uncertainty in the Kalman filter for a sonar based positioning system. Proc 8<sup>th</sup> Int Symp on Unmanned Untethered Submersible Technology, p.405.
- Bowen AD, Yoerger DR, Taylor C, et al., 2009. Field trials of the Nereus hybrid underwater robotic vehicle in the Challenger Deep of the Mariana Trench. OCEANS, p.1-10. <https://doi.org/10.23919/OCEANS.2009.5422311>
- Fofonoff NP, Millard RC, 1983. Algorithms for computation of fundamental properties of seawater. *UNESCO Tech Pap Mar Sci*, 44:1-53.
- Gardner JV, Armstrong AA, Calder BR, et al., 2014. So, how deep is the Mariana Trench? *Mar Geod*, 37(1):1-13. <https://doi.org/10.1080/01490419.2013.837849>
- Han YR, Wang B, Deng ZH, et al., 2017. A mismatch diagnostic method for TERCOM-based underwater gravity-aided navigation. *IEEE Sens J*, 17(9):2880-2888. <https://doi.org/10.1109/JSEN.2017.2685429>
- Kyo M, Hiyazaki E, Tsukioka S, et al., 1995. The sea trial of "KAIKO", the full ocean depth research ROV. OCEANS, p.1991-1996. <https://doi.org/10.1109/OCEANS.1995.528882>
- Li S, Zeng J, Wang Y, 2011. Navigation under the arctic ice by autonomous & remotely operated underwater vehicle. *Robot*, 33(4):509-512 (in Chinese). <https://doi.org/10.3724/SP.J.1218.2011.00509>
- McDougall TJ, Barker PM, 2011. Getting Started with TEOS-10 and the Gibbs Seawater (GSW) Oceanographic Toolbox. SCOR/IAPSO WG127, ISBN 978-0-646-55621-5.

- Nakajoh H, Murashima T, Sugimoto F, 2018. Development of full depth fiber optic cable ROV (UROV11K) system. *OCEANS*, p.1-8. <https://doi.org/10.1109/OCEANS.2018.8604795>
- Sea-Bird Electronics Inc., 2007. SEASOFT-Win32: SBE Data Processing. <https://www.seabird.com/asset-get.download.jsa?code=251446>
- Tang YG, Wang J, Lu Y, et al, 2019. Parametric design method and experimental research on Haidou full-depth ocean autonomous and remotely-operated vehicle. *Robot*, 41(6):697-705 (in Chinese). <https://doi.org/10.13973/j.cnki.robot.180684>
- Wang HB, Xu XS, Zhang T, 2018. Multipath parallel ICCP underwater terrain matching algorithm based on multibeam bathymetric data. *IEEE Access*, 6:48708-48715. <https://doi.org/10.1109/ACCESS.2018.2866687>
- Wang KD, Yong Y, 2010. Influence of application conditions on terrain-aided navigation. *Proc 8<sup>th</sup> World Congress on Intelligent Control and Automation*, p.391-396. <https://doi.org/10.1109/WCICA.2010.5555067>
- Yuan GN, Zhang HW, Yuan KF, et al., 2012. Improved SITAN algorithm in the application of aided inertial navigation. *Int Conf on Measurement, Information and Control*, p.922-926. <https://doi.org/10.1109/MIC.2012.6273436>
- Zhao L, Gao N, Huang BQ, et al., 2015. A novel terrain-aided navigation algorithm combined with the TERCOM algorithm and particle filter. *IEEE Sens J*, 15(2):1124-1131. <https://doi.org/10.1109/JSEN.2014.2360916>